Enhanced H-mode pedestals with increased density fluctuations during lithium aerosol injection in DIII-D

Z. Yan[1], G.R. McKee[1], T.H. Osborne[2], G.L. Jackson[2], R. Maingi[3], D.K. Mansfield[3], A.L. Roquemore[3], B.A. Grierson[3], C.P. Chrobak[4], A.G. McLean[5], S.L. Allen[5], D.J. Battaglia[3], A.R. Briesemeister[6], M.Fenstermacher[5], P.B. Snyder[2], and the DIII-D team

[1] University of Wisconsin-Madison, Madison, WI, USA
[2] General Atomics, San Diego, CA, USA
[3] Princeton Plasma Physics Laboratory, Princeton, NJ, USA
[4] University of California, San Diego, San Diego, CA, USA
[5] Lawrence Livermore National Laboratory, Livermore, CA, USA
[6] Oak Ridge National Laboratory, Oak Ridge, TN, USA

Periods of ELM free H-mode (up to 350ms) with increased pedestal pressure and width were observed in the DIII-D tokamak when lithium particles were injected into the plasma. These periods are associated with enhanced density fluctuations (named 'Bursty Chirping Mode' in the later discussion) localized to the pedestal region. The dramatically increased fluctuations are shown to drive outward cross-field particle transport, which reduced the pressure gradient just inside the separatrix. This allowed higher overall pedestal pressure (twice that of normal H-modes) because of the improved peeling-ballooning stability limit.

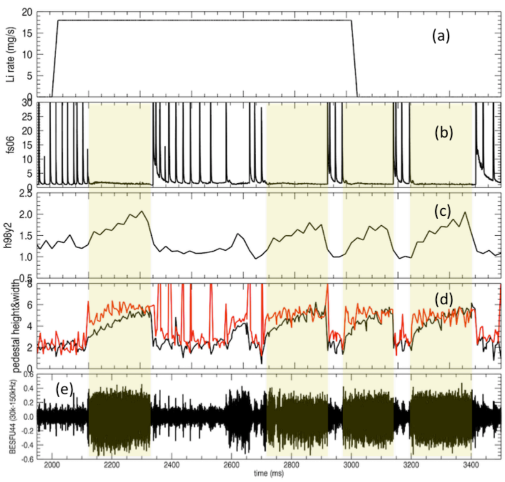

Fig. 1. Experimental parameters for shot 157267 with Li injection, (a) Lithium injection rate; (b) Dα light; (c) $H_{98y,2}$; (d) pedestal height (black) and width (red); (e) density fluctuations from the pedestal region from BES measurements. Periods of increased pedestal and density fluctuations are marked with the yellow bands.

The discharges were operated in a lower single null plasma shape with I_p=1.2MA, B_t=2.0T, q_{95}=4.4 and average triangularity ~0.5. Line average electron density was in the range of 3.4-4.7 x10^{19} m^{-3}. Li was injected into the plasmas as an aerosol of ~44 μm diameter particles from a Li dropper device located on the top of the DIII-D tokamak. Details of the injector hardware can be found elsewhere [1]. Lithium injection rates of 9-90 mg s^{-1} were used, corresponding to 3.8×10^5-3.8×10^6 particles per second or 7.8×10^{20}-7.8×10^{21} atoms s^{-1}. In comparison, a typical DIII-D discharge (assuming Z_{eff}=1.5, ne=6×10^{19} m^{-3}, plasma volume=21m^3) contains ~10^{21} deuterons. As shown in Fig.1, periods of enhanced ELM-free H-mode were observed (marked with the yellow bands) with Li aerosol injection at a rate of 18mg s^{-1} (Fig.1 (a)). $H_{98y,2}$ (Fig.1 (c)), pedestal pressure height and width (Fig.1 (d)) all increase during the ELM free phases.

Density fluctuations were measured with a 2D array of high sensitivity Beam Emission Spectroscopy (BES) [2] located across the pedestal region from ψ_N~0.88-1.06. As is shown in Fig. 1(e) density fluctuations from the pedestal region increase dramatically during the enhanced ELM-free phases. Fig. 2 is a spectrogram of such density fluctuations near ψ_N~0.995. The frequency of such fluctuations spans from ~40kHz-150kHz. Notably the spectra exhibit a moderately broad frequency width on the time scale of hundreds of ms. However, when inspected on a time scale of a few ms, these fluctuations are bursty in time with each burst lasting a few hundred μs. Within each burst the frequency of the modes changes rapidly both up and down, while the mode itself appears coherent on very short time scales [3]. This is qualitatively different from the broadband turbulence that is typically observed in the pedestal region of H-mode plasmas [4]. Given the rapidly bursting and frequency shifting nature, these modes with Li injection have been named as the 'Bursty Chirping Mode' (BCM).

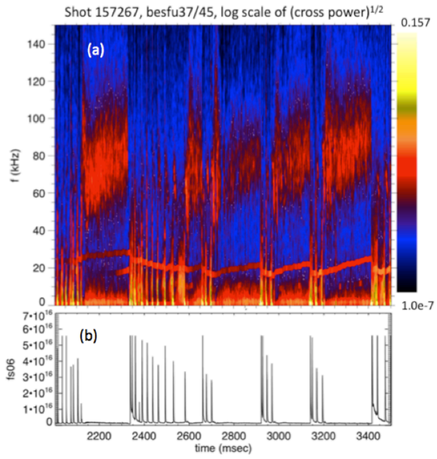

Fig. 2 (a) Spectrogram of density fluctuations from BES at ψ~0.995 for shot 157267 with Li injection; (b) edge D_α light.

The onset of the BCM occurs rapidly, typically within 10 ms after an ELM crash. The poloidal wave number of the BCM is k_θ~0.5 cm^{-1} with $k_\theta\rho_s$~0.1-0.2. Fig.3 is a radial profile of the relative density fluctuation amplitudes of these modes as a function of ψ_N from BES measurements integrated over 40-150kHz, where the BCM is observed. The modes are localized to the pedestal region and peak just inside the separatrix. The peak amplitude is nearly ñ/n~8%. This exceeds by ~ tenfold the typical pedestal fluctuations observed in normal H-modes in between ELMs. The modes propagate in the electron diamagnetic direction in the plasma frame [3], consistent with the trapped electron mode (TEM) or micro-tearing mode characteristic. The poloidal correlation length is about 10cm, while the radial correlation length is less than 3cm, showing a strong spatial asymmetry to the mode structure.

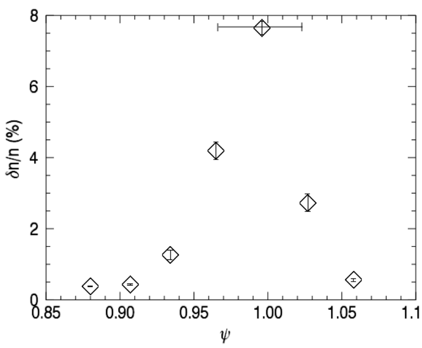

Fig. 3. Radial profiles of relative density fluctuation amplitude integrated over 40kHz to 150kHz from BES measurements.

The time scale of pedestal expansion correlates with the time scale for the growth of the BCM from the BES measurements. During the BCM, each burst correlates well with an increase of the C-III light at both the outer and inner divertor strike point locations, suggesting that the BCM increases plasma loss to the divertor [3]. This can be directly demonstrated from the experimentally inferred particle flux by applying a velocimetry technique to the 2D BES measurements [5]. This technique has the merit of obtaining the velocity field at the sampling time for BES (1 μs) to capture the fast flow dynamics of the turbulent eddy structures. By comparison, the decorrelation time for BCM is of order several μs. Fig. 4 is an example of a set of 2D density fluctuation images with time interval of 1 μs. It shows that the BCM density perturbation propagates in the electron diamagnetic direction (downwards in the image) and outwards. With the measured instantaneous fluctuating radial velocity, the inferred radial particle flux can thus be calculated as $\Gamma = \tilde{n}_e \tilde{V}_r$. Figure 5 are joint probability distribution functions (PDFs) of $\tilde{V}_r$ and $\tilde{n}_e$ at two radial locations, ψ_N~0.965 (Fig.5 (a)) and ψ_N~0.88 (Fig.5 (b)). The dashed lines on both figures are zeros of $\tilde{V}_r$ and $\tilde{n}_e$, distributing the figure into four quadrants. It shows that at ψ_N~0.965 there are more events in the 1st (upper right section of the figure) and 3rd (lower left section of the figure) quadrant than those at ψ_N~0.88, indicating that more positive density perturbations with outward going (positive $\tilde{V}_r$) events and negative density perturbations with inward going (negative $\tilde{V}_r$) events take place, reflecting on average an outward flux. Fig. 5(c) is a PDF of inferred particle flux, Γ, at ψ~0.965. It shows a significant positive skewed PDF indicating intermittent or bursty particle transport events which are characterized by outward-going positive density perturbations. Fig. 6 shows the radial profile of the skewness of the inferred particle flux [i.e., the skewness is the third moment of the probability distribution function measuring the asymmetry of the distribution of the signal, defined as $\Gamma^3 / \langle \Gamma^2 \rangle^{1.5}$]. A comparison of Fig. 3 and Fig. 6 shows that the location where the skewness of particle flux is

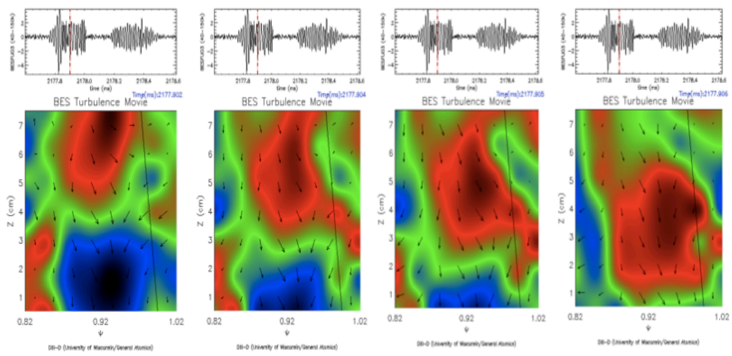

Fig.4 2D images of density fluctuation from BES measurements. Time interval is 1us. Black solid line on each image is the separatrix. Red color indicates positive density perturbations and blue color indicates negative density perturbations.

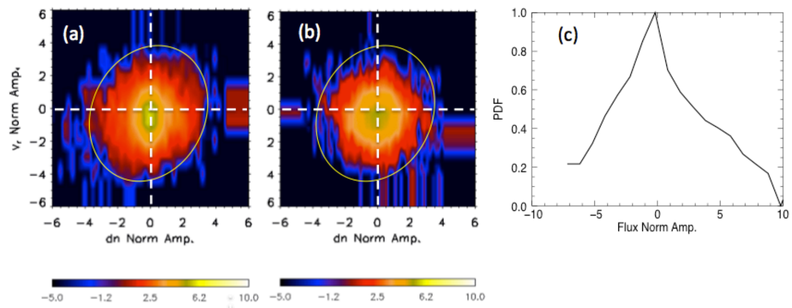

Fig.5 Joint PDF of $\tilde{V}_r$ and $\tilde{n}_e$ at (a) ψ~0.965 and (b) ψ~0.88; (c) PDF of inferred particle flux at ψ~0.965; White dashed lines on (a) and (b) are zero line of $\tilde{V}_r$ and $\tilde{n}_e$. Elliptical lines are exact the same on both (a) and (b) to help comparison.

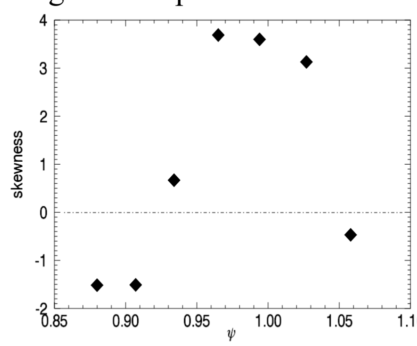

Fig. 6 Skewness of inferred particle flux from BES measurements.

significantly positive is where the amplitude of BCM is maximal. This asymmetry of the skewness across the pedestal and the alignment with the pedestal pressure profile demonstrates that BCM drives outward particle transport that could impact the pedestal profile evolution. This indeed has been shown from the correlation between the initiation and termination of the BCM and the profile evolution during an ELM-free phase [3]. At the BCM onset there is a reduction in electron density and perhaps also temperature in the region near the separatrix where BCM locates. The reduction persists while the BCM is present, and the pedestal continues to expand inboard of this region. When the BCM terminates both temperature and density profiles rebuild near the separatrix. This BCM-induced local flattening of the pressure gradient near the separatrix allows an increased pedestal pressure within the MHD stability constraints. It has been shown that in the Li diluted with BCM present periods the plasmas are operated well below the PBM limit [3].

In summary, significantly enhanced H-mode pedestal pressure and global energy confinement were observed in DIII-D discharges with a small amount of Li injection when large amplitude density fluctuations, the BCM, were present. The modes drive outward particle transport flattening local pressure gradient near separatrix, which allows wider pedestal width and higher pedestal pressure at improved PBM stability. Gyrokinetic simulations will be carried out to attempt to identify the nature and instability of the observed mode, as well as possible connection to a coherent mode observed in EAST during Li injection [6].

This material is based upon work supported by the U.S. DOE, under Awards DE-FG02-89ER53296, DE-FC02-04ER54698, DE-AC02-09CH11466, DESC0012551, DE-FG02-07ER54917, DE-AC52-07NA27344 and DE-AC05-00OR22725.

Reference:

[1] D. Mansfield, et al Fusion Eng. Des. **85**, 890, 2010

[2] G. McKee, et al Rev. Sci. Instrum., **81**, 10D741, 2010

[3] T. Osborne, Nuclear Fusion, **55**, 063018, 2015

[4] Z. Yan, Physics of Plasmas, **18**, 056117, 2011

[5] G. McKee, Rev. Sci. Instrum, **75**, 3490, 2004

[6] J.S. Hu, et. al., Phys. Rev. Letts. **114**, 055001, 2015